1.36 million years of Mediterranean forest refugium dynamics in response to glacial–interglacial cycle strength

Timme Donders[a,1], Konstantinos Panagiotopoulos[b], Andreas Koutsodendris[c], Adele Bertini[d], Anna Maria Mercuri[e], Alessia Masi[f], Nathalie Combourieu-Nebout[g], Sébastien Joannin[h], Katerina Kouli[i], Ilias Kousis[c], Odile Peyron[h], Paola Torri[e], Assunta Florenzano[e], Alexander Francke[j], Bernd Wagner[b], and Laura Sadori[f]

[a]Palaeoecology, Department of Physical Geography, Utrecht University, 3584 CB, Utrecht, The Netherlands; [b]Institute of Geology and Mineralogy, University of Cologne, 50674 Köln, Germany; [c]Institute of Earth Sciences, Heidelberg University, D-69120 Heidelberg, Germany; [d]Dipartimento di Scienze della Terra, Università di Firenze, 50121 Firenze, Italy; [e]Laboratorio di Palinologia e Paleobotanica, Dipartimento di Scienze della Vita, Università di Modena e Reggio Emilia, 41125 Modena, Italy; [f]Dipartimento di Biologia Ambientale, Università di Roma La Sapienza, UMR 7194-HNHP Rome, Italy; [g]Centre National de la Recherche Scientifique, Departement Homme et Environnement, Muséum national d'Histoire naturelle, Institut de Paléontologie Humaine, F75013 Paris, France; [h]Institut des Sciences de l'Evolution de Montpellier, Université de Montpellier, CNRS, Ecole pratique des hautes études, 34090 Montpellier, France; [i]Faculty of Geology and Geoenvironment, National and Kapodistrian University of Athens, 15784, Athens, Greece; and [j]Department of Earth Sciences, University of Adelaide, North Terrace, SA 5005, Australia

Edited by Cathy Whitlock, Montana State University, Bozeman, MT, and approved June 28, 2021 (received for review December 18, 2020)

The sediment record from Lake Ohrid (Southwestern Balkans) represents the longest continuous lake archive in Europe, extending back to 1.36 Ma. We reconstruct the vegetation history based on pollen analysis of the DEEP core to reveal changes in vegetation cover and forest diversity during glacial–interglacial (G–IG) cycles and early basin development. The earliest lake phase saw a significantly different composition rich in relict tree taxa and few herbs. Subsequent establishment of a permanent steppic herb association around 1.2 Ma implies a threshold response to changes in moisture availability and temperature and gradual adjustment of the basin morphology. A change in the character of G–IG cycles during the Early–Middle Pleistocene Transition is reflected in the record by reorganization of the vegetation from obliquity- to eccentricity-paced cycles. Based on a quantitative analysis of tree taxa richness, the first large-scale decline in tree diversity occurred around 0.94 Ma. Subsequent variations in tree richness were largely driven by the amplitude and duration of G–IG cycles. Significant tree richness declines occurred in periods with abundant dry herb associations, pointing to aridity affecting tree population survival. Assessment of long-term legacy effects between global climate and regional vegetation change reveals a significant influence of cool interglacial conditions on subsequent glacial vegetation composition and diversity. This effect is contrary to observations at high latitudes, where glacial intensity is known to control subsequent interglacial vegetation, and the evidence demonstrates that the Lake Ohrid catchment functioned as a refugium for both thermophilous and temperate tree species.

Pleistocene | pollen | glacial–interglacial cycles | tree diversity | vegetation dynamics

Identification and protection of past forest refugia, supporting a relict population, has gained interest in light of projected forest responses to anthropogenic climate change (1–4). Understanding the past and present composition of Mediterranean forest refugia is central to the study of long-term survival of tree taxa and the systematic relation between forest dynamics and climate (5). The Quaternary vegetation history of Europe, studied for over a century, is characterized by successive loss of tree species (6–8). Species loss was originally explained by the repeated migration across east–west oriented mountain chains during glacial–interglacial (G–IG) cycles (9). Later views gave more importance to the survival of tree populations during warm and arid stages in southern refugia (10, 11). Tree survival likely depends on persistence of suitable climate and tolerable levels of climate variability, as well as niche differentiation and population size at the refugium (12), although the precise relation between regional extinctions, climate variability, and local edaphic factors is not well known (13). Mediterranean mountain regions are considered to serve as forest refugia over multiple glacial cycles and frequently coincide with present-day biodiversity hotspots (14). Across the Mediterranean, increases in aridity and fire occurrence have impacted past vegetation communities (15–18). Comprehensive review of available Quaternary Mediterranean records indicates that Early (2.58 to 0.77 Ma) and Middle Pleistocene (0.77 to 0.129 Ma) tree diversity was higher compared to the present (13, 19–21). Particularly drought intolerant, thermophilic taxa were more abundant and diverse (8) but with strong spatial and temporal variations in tree diversity across the region. Long-term relationships between refugia function and environmental change over multiple G–IG cycles are hard to quantify due to the rarity of long, uninterrupted records.

Significance

Forest conservation and restoration are important means to counter threats caused by habitat fragmentation and global change. Diverse and resilient forests can only be maintained if we understand their sensitivity to past climate change. The sedimentary record of the oldest extant lake in Europe, Lake Ohrid (North Macedonia, Albania), shows the survival and extinction of tree species during glacial and interglacial stages (G–IG) of the Quaternary. Pollen analysis reveals that the area was an effective refuge for tree populations through G–IG periods. The lake body locally buffered the climate, allowing repeated recovery of tree populations that were close to disappearance. However, extended periods of aridity during G–IG intensification after 0.94 Ma caused many tree taxa to disappear.

Author contributions: T.D., B.W., and L.S. designed research; T.D., K.P., A.K., A.B., A.M.M., A.M., N.C.N., S.J., K.K., I.K., P.T., A. Florenzano, and L.S. performed research; T.D., K.P., A.K., A.B., A.M.M., A.M., N.C.N., S.J., K.K., I.K., O.P., A. Francke, B.W., and L.S. analyzed data; and T.D., K.P., A.K., A.B., A.M.M., A.M., N.C.N., S.J., K.K., A. Francke, B.W., and L.S. wrote the paper.

The authors declare no competing interest.

This article is a PNAS Direct Submission.

[1]To whom correspondence may be addressed. Email: t.h.donders@uu.nl.

This article contains supporting information online at https://www.pnas.org/lookup/suppl/doi:10.1073/pnas.2026111118/-/DCSupplemental.

Published August 16, 2021.

The Early–Middle Pleistocene Transition (EMPT), between 1.4 and 0.4 Ma (22), is of particular importance for understanding the relation between past climate change, vegetation dynamics, and biodiversity in the Mediterranean region. The EMPT is characterized by a gradual transition of G–IG cycle duration from obliquity (41 thousand years; kyr) to eccentricity (100 kyr) scale with increasing amplitude of each G–IG cycle (e.g., refs. 23, 24). The EMPT was accompanied by long-term cooling of the deep and surface ocean and was likely caused by atmospheric CO_2 decline and ice-sheet feedbacks (25–30). In Europe, the EMPT is associated with pronounced vegetation changes and local extinction and isolation of small tree populations (31).

Here, we document vegetation history of the last 1.36 Ma in the Lake Ohrid (LO) catchment, located at the Albanian/North Macedonian border at 693 m above sea level (m asl, Fig. 1), the longest continuous sedimentary lake record in Europe (32, 33). The chronology of the DEEP core (International Continental Scientific Drilling Program site 5045-1; 41°02'57" N, 20°42'54" E, Fig. 1) is based on tuning of biogeochemical proxy data to orbital parameters with independent tephrostratigraphic and paleomagnetic age control (32, 33). The Balkan Peninsula has long been considered an important glacial forest refugium for presently widespread taxa such as *Abies*, *Picea*, *Carpinus*, *Corylus*, *Fagus Ostrya*, *Quercus*, *Tilia*, *and Ulmus* (7, 34–36). More than 60% of the Balkans is currently located >1,000 m asl (36), providing steep latitudinal and elevational gradients to support refugia under both cold and warm conditions. Today, the LO catchment is dominated by (semi) deciduous oak (*Quercus*) and hornbeam (*Carpinus*/*Ostrya*) forests. Above 1,250 m elevation, mixed mesophyllous forest with montane elements occurs (*Fagus* and at higher elevations *Abies*), which above 1,800 m elevation develops into subalpine grassland with *Juniperus* shrubs (see ref. 37 for site details). Isolated populations of *Pinus peuce* and *Pinus nigra* currently grow in the area (37–40).

Previous analysis of pollen composition of the last 500 kyr at the DEEP site revealed that the LO has been an important refugium. Arboreal pollen (AP) is deposited continuously and changes in abundance on multimillennial timescales in association with G–IG cycles, whereas millennial-scale variability is tightly coupled to Mediterranean sea-surface temperature variations (37, 41–45). Subsequent studies confirm the refugial character of the site recording Early Pleistocene (1.365 to 1.165 Ma) high relict tree diversity and abundance—and significant hydrological changes, including an increase in lake size and depth (38). Here, we present a continuous palynological record from LO with millennial resolution (~2 kyr) back to 1.36 Ma to assess the systematic relationships between tree pollen abundance, forest diversity, and G–IG climate variability.

Our objective is as follows: 1) infer the impact of past climate variability on local vegetation across the EMPT, 2) estimate tree species diversity in the catchment, and 3) examine how the amplitude and duration of preceding G–IG intervals affected the vegetation development and plant species diversity in this refugial area.

Results and Discussion

Vegetation Responses to Basin Development and G–IG Dynamics. The DEEP pollen record was divided into pollen superzones that reflect G–IG cycles (labeled OD-1 to OD-40; *SI Appendix*, Table S1 and Fig. S1), following the approach of Sadori et al. (37, 41). These G–IG variations are characterized by alternations between AP (AP %) and herbs (nonarboreal pollen; NAP %) (Fig. 2), superimposed on a long-term trend toward more herbs and shrubs (*SI Appendix*, Figs. S3 and S4).

The pollen data indicate two phases of major vegetation reorganizations (Fig. 2). Prior to the first transition at 1.16 Ma (OD-31/32), trees were abundant during the majority of glacial cycles (only four samples have AP <40% before 1.16 Ma), which is in contrast to subsequent glacial stages with frequent AP values of 20 to 30%. Similarly, interglacial herb percentages rose across the 1.16 Ma transition (typical NAP <5% increased to 15 to 20%), after which steppic herb associations (Poaceae, *Artemisia,* Amaranthaceae, and Asteroideae) and semiarid shrubs zones established (mainly Cupressaceae and *Hippophaë*). Forest composition during the early lake phase (1.36 to 1.16 Ma) was characterized by abundant *Quercus cerris*–type, *Cedrus*, *Tsuga*, *Carya*, and *Picea*, relatively low *Pinus*, and above-average levels of *Corylus*, *Fagus*, *Liquidambar*, and *Pterocarya* (*SI Appendix*, Figs. S1 and S3 and Table S1). Palynological, biomarker, diatom, and geochemical data suggest a gradual expansion and deepening of the lake during the first 100 kyr of its existence (1.365 to 1.265 Ma), which resulted in the inundation of extensive wetlands surrounding the lake (38, 46). The low herb abundances during interglacials prior to 1.16 Ma suggest largely closed forest cover with no extensive herb associations in the catchment. Following the Early Pleistocene (OD-39 to OD-33; Marine Isotope stage [MIS] 42 to 36), when the Ohrid catchment was rather forested and the soil composition was stable (38), an increase in herb percentages during the OD-31 (MIS 34) records an opening of the landscape, considering that extensive wetland areas were inundated with the expansion and deepening of the lake during these early G–IG cycles (38). This rapid increase in *Artemisia* and Amaranthaceae percentages in OD-31 was most likely associated with a threshold response to glacial conditions since preceding glacials did not cause similarly strong vegetation shifts. This initial appearance of a steppic herb association after 1.16 Ma

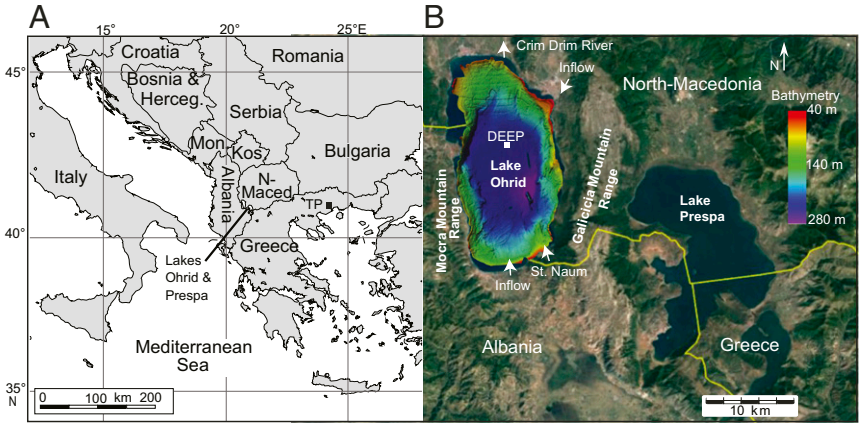

Fig. 1. (*A*) Location of LO and TP on the Balkan Peninsula. (*B*) Local setting around LO, bathymetry (81), and DEEP coring site (adapted from ref. 32).

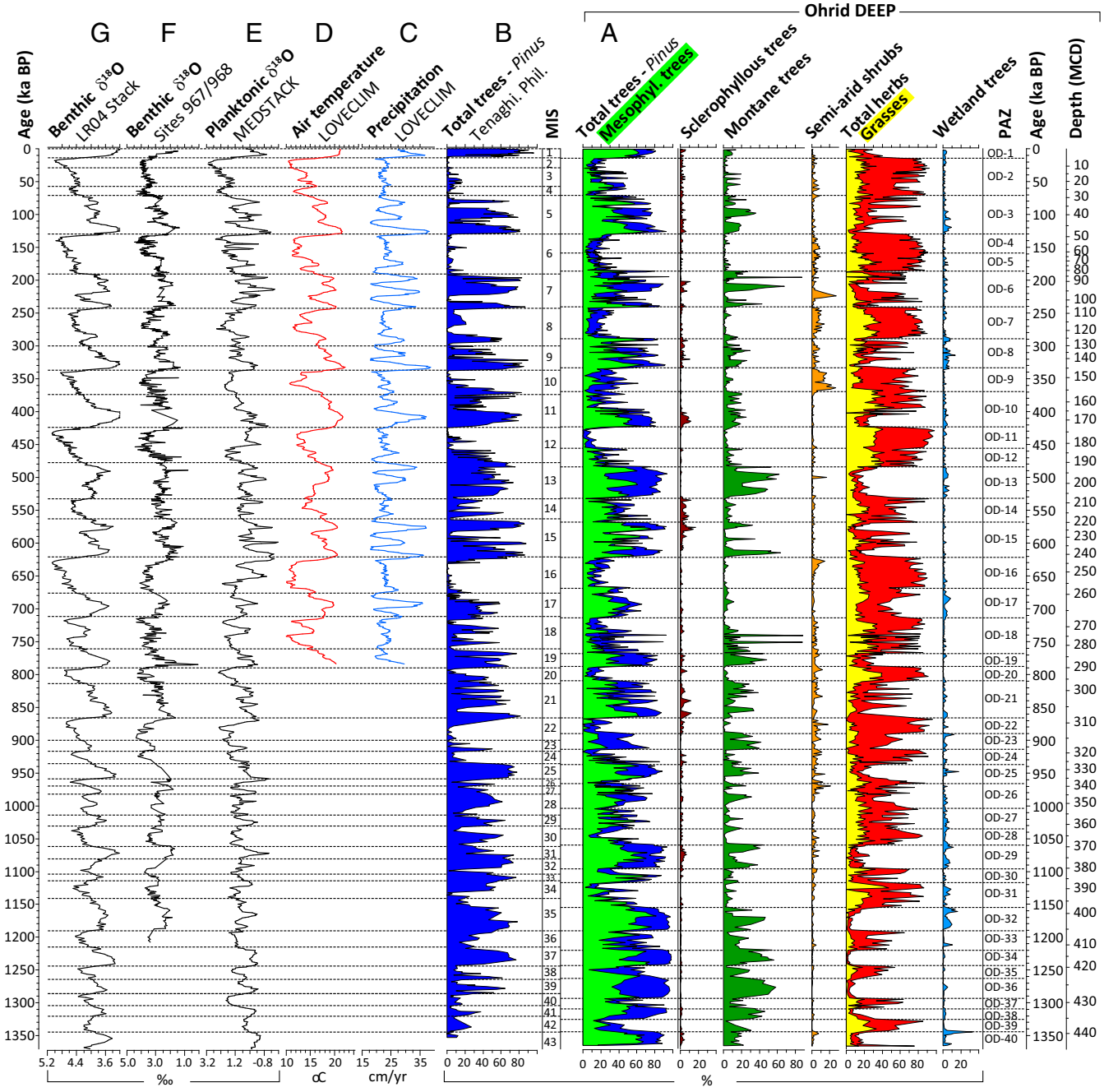

Fig. 2. (*A*) Pollen diagram of ecological groups (%) against chronology of Wagner et al. (33): montane trees (*Abies*, *Betula*, *Cedrus*, *Fagus*, *Ilex*, *Picea*, *Taxus*, *Tsuga*); mesophyllous trees (*Acer*, *Buxus*, *Carpinus betulus, Carya*, *Castanea*, *Celtis*, *Corylus*, *Fraxinus excelsior/oxycarpa*, *Hedera*, *Ostrya/Carpinus orientalis, Pterocarya*, *Q. cerris*–type, *Q. robur*–type, *Tilia*, *Ulmus*, *Zelkova*); Sclerophyllous trees (*Arbutus*, *Cistus*, *Fraxinus ornus*, *Olea*, *Phillyrea*, *Pistacia*, *Quercus ilex*–type, *Rhamnus*); wetland trees (*Alnus*, *Liquidambar*, *Platanus*, *Populus*, *Salix*, *Tamarix*, *Taxodium*-type); and semiarid shrubs (*Ephedra*, Ericaceae, *Hippophaë*, Cupressaceae [mostly *Juniperus*-type]). (*B*) TP (location see Fig. 1): AP percentages excluding *Pinus*, *Betula*, and *Juniperus*-type (55–58, 60). (*C*) Model timeseries of annual precipitation and (*D*) mean SAT for the LO grid cell (33, 67). (*E*) MEDSTACK planktonic $\delta^{18}O$ data (82). (*F*) Stacked benthic $\delta^{18}O$ data for Ocean Drilling Program sites 967 and 968 from the eastern Mediterranean (83). (*G*) LR04 $\delta^{18}O$ global benthic stack (24).

is consistent with independent evidence of a trend to more aridity in the Mediterranean region (21). At the same time, the Greek Tenaghi Philippon (TP, Figs. 1 and 2) pollen record shows a less pronounced shift to more herbs, suggesting an additional local-scale driver of intensified aridity at LO. Fossil diatom analysis (38, 46) places the shift to steppe vegetation in a period of lake deepening. Graben formation due to northeast–southwest geologic extension since the Pliocene likely drove the lake deepening and was accompanied by regional uplift (47). This uplift could explain part of the herb increase at LO by increasing the elevational vegetation gradient in the region and strengthening the aridity-driven reduction in forest cover, but this scenario requires further study.

The second transition at 0.94 Ma (OD-24/25) shows an increase in G–IG vegetation variability, characterized by reduced mesophyllous tree abundances during glacial periods (<10% compared to ~20% prior to the transition). High G–IG contrasts in vegetation prevailed after 0.94 Ma, except for OD-14 (MIS 14), which was a weakly developed glacial period (30). *Artemisia*

abundance, indicative of cool-arid conditions in montane settings (48), increased in post-0.94 Ma glacials, reaching ~30 to 40% during the most recent glacial stages (MIS 6 and 2 to 4; *SI Appendix*, Fig. S1) (37, 41). Semiarid shrubs (Fig. 2) were more abundant in herb-dominated samples with relatively low Poaceae abundance. *Abies* became more abundant post-0.94 Ma, reaching notable maxima at about 0.5 Ma (OD-13) and 0.2 Ma (OD-6). *Cedrus* abundance declined with each G–IG cycle after 0.94 Ma (*SI Appendix*, Fig. S1). *Q. cerris*–type abundance was higher in many, but not all, interglacials following the transition, relative to the 1.16 to 0.94 Ma period. Montane tree abundances were highly variable and, following the definition of Tzedakis et al. (49), occur principally during relatively cool (phases of) interglacials, such as in OD-6 (MIS 5a/c)—and OD-13 (MIS 13) (Fig. 2). Mediterranean tree taxa, commonly underrepresented in pollen data (21), were relatively low in abundance throughout the sequence but reached values of ~10% in zones OD-6, -10, -14, -15, and -21. Most of these phases were concurrent with insolation maxima (precession minima, *SI Appendix*, Fig. S4).

The full record extends the observed relationship between AP/NAP changes (37) and global and Mediterranean stacks of benthic marine oxygen isotopes (24, 50) back to 1.36 Ma. The insolation threshold for deglaciation increased during the EMPT (30), leading to eccentricity-paced glaciations (25, 26). The increased contrast in abundance and longer duration of forest and steppe periods are a clear expression of the EMPT (Fig. 2 and *SI Appendix*, Fig. S6). MIS 24 to 22 (~0.94 to 0.86 Ma) is considered the first prolonged eccentricity-paced glacial cycle (28) and was associated with a prolonged phase of high herb abundance (NAP 30 to 90%) and an unprecedentedly long (>50 ky) period of low (<30%) mesophyllous taxa at LO (zones OD-24 to OD-22). Although glacial vegetation composition and G–IG amplitude increases are evident, changes in the interglacial vegetation composition following the EMPT are less obvious (*SI Appendix*, Figs. S1 and S3). A key characteristic of the LO record is the clear precession-scale variability in mesophyllous tree abundance, particularly for deciduous oaks, which was driven by regional atmospheric teleconnections that resulted in phases of high winter rainfall during precession minima (33, 50) (*SI Appendix*, Fig. S6). The vegetation response to this forcing is particularly clear post-EMPT in interglacial periods MIS 5, 7, 9, and 13 and contrasts with the low-amplitude precessional forcing and the corresponding low mesophyllous variability in MIS 11 and 19 (Fig. 2 and *SI Appendix*, Fig. S4). High precession amplitude during glacials (e.g., MIS 8 and 6) did not lead to a similar expansion of mesophyllous forest, suggesting that during glacials the precession-forced humidity increases were not enough to alter vegetation. Although a vegetation response to changes in precession is evident in the entire sequence (ref. 33; *SI Appendix*, Fig. S6), cross correlation results show that phase relations between individual tree taxa vary over time (*SI Appendix*, Fig. S6), reflecting a change in vegetation patterns as a result of intensification of G–IG cycles. Prior to 0.94 Ma, the *Abies* maxima lagged deciduous oaks by >12 kyr and, together with NAP and *Pinus*, primarily displayed low-amplitude variation characteristic of obliquity-forced G–IG cycles. In contrast, the timing of *Abies* became closer to the deciduous oak maxima (mean offset of 6 kyr) between 0.94 Ma to present (*SI Appendix*, Fig. S6) consistent with a more pronounced vegetation change from forest to steppe, characteristic of stronger, eccentricity-paced G–IG cycles. Similarly, *Pinus* abundance gradually varied across the EMPT with high values during glacial maxima and an antiphased relation to deciduous oak before 0.94 Ma, to mostly interglacial abundance maxima in the last 0.5 My. Together with *Abies*, *Pinus* varied on precession timescales in this later phase with a 6 kyr offset relative to deciduous oaks (*SI Appendix*, Fig. S6). A commonly observed increase of deciduous oaks prior to late successional taxa, such as *Carpinus* (5), was not seen at LO, which likely reflects its refugium character and relative lack of vegetation change within interglacials.

Relict Tree Abundance and Regional Trends. The Ohrid DEEP record shows high abundance and diversity of tree taxa (Fig. 3) that are currently extinct in mainland Europe, or occur as relict populations on Mediterranean islands, in western Asia, and/or North Africa (8, 31). The assemblages also include extant taxa that were locally rare or absent at LO during much of the Pleistocene, such as *Fagus* and *Juglans*. Between 1.36 to 1.16 Ma, primarily *Cathaya*, *Cedrus*, *Tsuga*, *Eucommia*, *Carya*, *Fagus*, *Liquidambar*, *Pterocarya*, and *Zelkova* were recorded (OD-40 to -32). From 1.16 Ma onwards, *Castanea*, *Buxus*, *Celtis*, Hamamelidaceae, *Taxodium*-type, and *Sequoia*-type established in the catchment, while *Cedrus* and *Fagus* decreased in abundance. In contrast to most other taxa, *Fagus* had a disjunct distribution of abundance before 0.92 Ma, followed by isolated occurrences and strong recovery during the last 100 kyr. A few other taxa show phases of recovery; *Cedrus* was present until 0.8 Ma, subsequently between 0.67 to 0.43 Ma, and between 0.13 to 0.03 Ma. *Pterocarya* was nearly absent between 0.72 to 0.53 Ma and, *Juglans*, *Castanea*, and *Buxus* were absent between 0.48 to 0.33 Ma (Fig. 3) after which they recovered. Most other relicts and rare taxa had a near-continuous presence until ~1.0 to 0.8 Ma (e.g., *Carya*, *Liquidambar*, *Pterocarya*, *Taxodium*-type, and *Tsuga*, *Zelkova*), after which they occurred in low frequencies during short phases of some interglacials and finally disappear.

Scattered occurrences might represent declining local populations, periods of vegetative growth with little or no production of pollen (e.g., ref. 51), and/or stands at greater distance such as from the Lake Prespa catchment (Fig. 1) that today has a slightly different forest composition (39, 40). Long-distance transport (52) or reworking might be additional causes for isolated pollen occurrences in single samples (42). No long-term decrease or systematic offset in count sums explains the major phases of taxa decline (*SI Appendix*, Table S1), and brief intervals of low abundances occur in subsequent samples, which supports the reliable detection of small tree populations in the analysis. The tephra horizons in the DEEP core are sourced to Italian volcanic provinces despite numerous potential eastern (Aegean, Anatolian) volcanic sources, consistent with dominant westerly winds (33, 42, 53). This information argues against a long-term shift in prevailing wind direction to explain the overall pollen abundance patterns. Sediment and diatom analysis and available chronostratigraphic information also exclude significant reworking of pollen grains (33, 54) but cannot be entirely ruled out.

In the context of regional patterns of Quaternary relict tree taxa (13), notable observations in the LO record include the near-continuous presence of *Taxodium*-type pollen until 1.0 Ma and between 0.92 to 0.85 Ma. Other continuous records of *Taxodium*-type only ranged until ~1.5 Ma, although scattered occurrences are known from central Italy and Greece until ~0.5 Ma (13). Likely the shallow early lake phase offered good habitat to some taxa of Taxioideae and other wetland trees such as *Liquidambar* and *Carya* (although *Carya* is not exclusively a wetland tree). The last occurrences (outside current relict populations) of *Cathaya* (0.85 Ma), *Cedrus* (0.03 Ma, discontinuous), and *Zelkova* (0.07 Ma) are most closely comparable to available Italian records (13), while the *Eucommia* presence after 1.1 Ma at LO is only otherwise known from the TP record in northeastern Greece (55–58) and, curiously, NW Europe (59). The TP record so far is the only continuous European pollen record of comparable length, dated to 1.35 Ma (60). The last occurrences of *Carya* (0.25 Ma), *Pterocarya* (0.4 Ma), and *Liquidambar* and *Tsuga* (0.7 Ma) at LO and TP occur at the same time, and *Carya* is also known from MIS 9 in central Italy (51). In high-resolution analyses of selected intervals from LO, scattered grains of *Tsuga* and *Parrotia* have been reported until 0.4 Ma (MIS 11), which significantly postdates

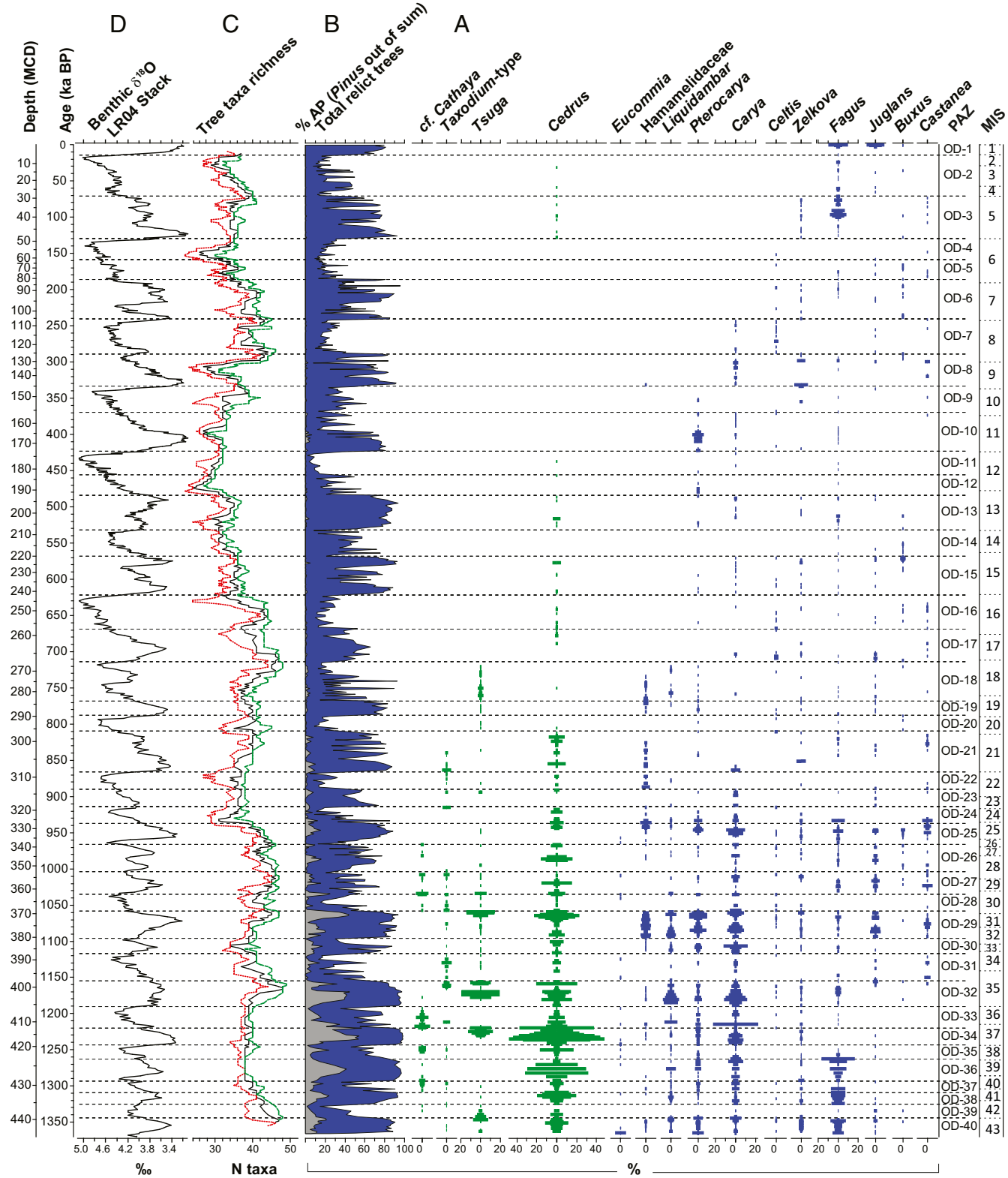

Fig. 3. Relicts and richness. (*A*) Range and relative abundance of relict tree taxa in the DEEP site of LO together with (*B*) total % AP (filled blue) and % total relict taxa (filled gray, excl. *Fagus*). Bars represent % abundances for relict and rare tree taxa and are mirrored to enhance visibility. (*C*) Tree taxa richness of the DEEP site is based on taxa accumulation curves of tree pollen along a moving window. Single data points represent total richness from SAC (see *Methods*) with a sliding window of size 10 (red dotted line), 15 (black line), or 20 (green dashed line). All LO data are plotted against the chronology of Wagner et al. (33). (*D*) LR04 $\delta^{18}O$ global benthic stack (24).

known occurrences of relict taxa in southern Europe and might represent long-distance transport or reworking (42).

Richness Variations and Intensification of G–IG Variability. The palynological richness of tree taxa, estimated by species accumulation curves (SAC) (Fig. 3), shows relatively high values (> 25 taxa) during the entire record in line with the suggested refugial character of the site and the surrounding region (37, 42, 43, 45). Tree richness before 0.94 Ma was high (>40 taxa) and relatively stable. Also, the relative abundance of relict tree taxa was high (>30% in interglacials) but, in contrast to the tree richness, the abundance covaried with marine benthic $\delta^{18}O$ G–IG cycles (24). High-resolution rarefaction analysis for the Early Pleistocene dataset from LO (1.365 to 1.165 Ma) (61), showed a gradual decline in total palynological richness within the first 100 kyr of lake existence followed by a stabilization for the rest of the interval (38). During the early development phase of LO, the palynological richness was possibly affected by declining landscape openness due to lake-level rise and receding wet meadows. However, the early decline is mirrored in our present analysis, which considers tree pollen only and uses the cumulative richness of consecutive samples to detect rare pollen occurrences (see *Methods*).

The tree richness record responds to the amplification and lengthening of G–IG cycles during the EMPT in several steps. Relict tree relative abundance (principally *Cedrus*) decreased sharply at 1.16 Ma related to the establishment of the permanent herb association from OD-31, while tree richness increased and became more variable (Fig. 3). Regional tectonic uplift (47) likely contributed to a stronger elevational gradient with increased vegetation differentiation and, as is observed for modern large lake basins (62, 63), potential development of a locally milder microclimate for diverse tree populations to persist despite the greater regional aridity. The first major decline in tree richness occurred at 0.94 Ma with the first prominent eccentricity-paced G–IG cycle, and most relict taxa show a discontinuity in their temporal range at that time (Fig. 3). Tree richness recovered over the next two G–IG cycles, followed by renewed decline between 0.7 and 0.5 Ma during the end of EMPT. Richness remained relatively stable and mostly well below 40 taxa until 0.35 Ma and subsequently recovered to 40 to 50 taxa (MIS 9 to 7), coincident with lower amplitude G–IG variability in benthic $\delta^{18}O$ (24). Tree richness after 0.2 Ma (MIS 6 to 1) returned to moderately variable, intermediate values of mostly <40 taxa (Fig. 3).

Regional tree taxa loss is evident during MIS 22 (northeastern Spain and southern France), MIS 16 (Greece and Aegean, northeastern Spain and southern France), MIS 20 to 14 (northern Italy), and MIS 12 (central/southern Italy) (13). Although these changes have not been quantified as richness estimates and represent composite records from multiple basins, the general pattern of taxa loss seen at LO during the EMPT is supported. Comparable to the LO record, TP shows maximum tree diversity prior to MIS 24 to 22 and a clear extended minimum after MIS 16, with no major extinctions during MIS 12 (60). A further similarity between these two records is low interglacial abundance of *Corylus* and *Fagus*. These similarities in the decline of tree diversity suggest that the signals at LO and TP are part of a regional trend.

The LO record shows that even during glacial periods, when forest vegetation belts were compressed and herb vegetation expanded, tree diversity remained high except in the most extensive glaciations, in support of the refugial characteristics of the catchment. Equally, pronounced interglacials (MIS 5e, 11c, and 31) had relatively little impact on tree richness. Although there is no one-to-one relation between tree richness and the amplitude or duration of G–IG cycles, long-term richness declines did not occur during interglacials (declines during MIS 4 to 3b, 7a to 6d, 9c, 12c, 16a, 19b, and 24). Strikingly, long-term (>20 kyr) recoveries also occurred exclusively during glacial and interstadial conditions, not interglacials (MIS 9b, 10b/a, 18d to a, and 21d to a, 30/29 transition), with the notable exception of MIS 35. The tree richness declines were associated with aridity-adapted herb associations (e.g., OD-2, -4, -16, and -24 with high *Artemisia* and Amaranthaceae, *SI Appendix*, Fig. S3), suggesting drought severity as an important driver in addition to G–IG temperature change. Conversely, glacials with no significant tree richness decline (e.g., OD-7, -11, and -20) generally had higher amounts of Poaceae and Cyperaceae, indicative of greater soil moisture. This pattern in moisture variability is also observed in stable isotope-based water balance reconstructions from LO back to 0.6 Ma (64). Svenning (8) recognized that greater drought tolerance favored the relatively late disappearance of *Tsuga*, *Eucommia*, *Carya*, and *Pterocarya* in Europe, which is consistent with the early disappearance of more drought-sensitive *Taxodium* at LO. *Tsuga* disappearance in the Italian Peninsula has been explained by drought (16) and associated wildfires (18). The strong tree richness recovery at LO during MIS 9 to 7 coincides with less extreme G–IG cycles (24), with relatively moist conditions (49, 65) and limited ice buildup (30).

The exact roles of temperature and moisture availability in the tree diversity decline are difficult to quantify due to lack of continuous independent records. Mediterranean sea-surface temperature variations show variations of up to 10 °C across G–IG cycles (66) suggestive of a dominant temperature control of vegetation composition on multimillennial timescales. Long climate model hindcasts (Fig. 2, refs. 33, 67) regressed against AP% confirm this pattern (modeled annual surface air temperature [SAT], r^2 = 0.40, >0.0001; total annual precipitation [TAP], r^2 = 0.10, >0.0001) but additionally show that moisture variability explains more variance in the AP% than temperature at precessional timescales (SAT, r^2 = 0.07, >0.0001; TAP, r^2 = 0.18, >0.0001), likely due to strong convective precipitation during enhanced insolation (33, 50). Modern pollen data (68) show that deciduous *Quercus* pollen (>10%) occur at minimum mean annual temperatures of >5 °C. Since deciduous oaks have been continuously present in the LO catchment for the last 1.36 My (*SI Appendix*, Fig. S1), this sets a lower limit for glacial temperatures for the entire record. Although temperature variation has been a primary control of G–IG vegetation patterns, the enhanced variability on precessional time scales in the latter half of the record (*SI Appendix*, Fig. S6) was likely controlled by moisture availability, which therefore also was an important factor in the gradual decline in tree richness.

Legacy Effects on Vegetation Composition and Richness. The mean composition of the LO record, reflected by the first axis of a Detrended Correspondence Analysis (DCA, *SI Appendix*, Figs. S3 and S4), shows a strong negative correlation with maximum marine benthic $\delta^{18}O$ stack values (24) (r = −0.84, *SI Appendix*, Fig. S5), which represents minimum global temperature and/or maximum global ice volume reached during each correlative pollen zone. Evidence of a potential legacy effect from previous glacial periods on subsequent interglacial vegetation composition, such as described for the high-latitude paleolake El'gygytgyn (69), is limited at LO (r = −0.49, *SI Appendix*, Fig. S5) and likely reflects the refugial character of the region. In contrast, the maximum interglacial marine benthic $\delta^{18}O$ stack values (24) have a relatively strong negative correlation with the composition of the subsequent glacial pollen assemblage (r = −0.71, *SI Appendix*, Fig. S5), indicating increased persistence of relative cool-adapted vegetation caused short cool phases during interglacials. This relation might represent a "cold refugium" behavior whereby relatively cool interglacial conditions promote the survival and subsequent expansion of cold-adapted vegetation elements during glacials. For tree richness, both the concurrent glacial (r = −0.55) and preceding maximum interglacial benthic $\delta^{18}O$ stack values have the most pronounced negative correlation (r = −0.59, *SI Appendix*, Fig. S5). This comparison suggests that maximum cooling in both glacials

and interglacials is important for tree population survival and, consequently, long-term forest diversity.

In summary, the shift to eccentricity-paced G–IG cycles during the EMPT appears responsible for the long-term decline in temperate tree species at LO, whereas diversity was able to recover during low-amplitude G–IG cycles. The changed dynamics also affected the phase relation of montane taxa with respect to maximum insolation forcing. The diversity signal varied between G–IG cycles of varying intensity and duration. Differences in G–IG temperature contrasts, moisture availability, and frequency of polar air outbreaks (70) were key factors in the vegetation history at LO. Precession forcing controlled organic matter production and deciduous oak abundance at LO by varying the length and severity of the dry season (33), which likely also affected the long-term species survival on G–IG time scales. Unique characteristics of the LO basin, especially its topography and the thermal buffer capacity of the large lake resulted in relatively high glacial AP% and a more effective forest refugium compared to the Drama Basin area (TP site in eastern Greece), which was more vulnerable to polar air outbreaks (71). The recorded moisture sensitivity sheds light on Mediterranean forest development in glacial and interglacial periods and provides context for assessing forest resilience to twenty-first century climate change (4) and long-term species survival (2).

Methods

Palynology Processing and Analysis. Quantitative pollen analysis of the Ohrid DEEP site down to the base of the permanent lake phase was carried out at 64-cm resolution (~1.9 kyr). A total of 697 sediment samples have been processed and analyzed for pollen and spores. Palynological processing followed standard procedures outlined by Faegri et al. (72), consisting of treatment of 1.0 to 1.5 g dry sediment with cold HCl (37%), cold HF (40%), and hot NaOH (10%) to dissolve carbonates, silicates, and humic acids, respectively. Residues were mounted in glycerin for analysis by transmitted light microscopy. Pollen identification and counting approach is described in detail in Sadori et al. (37, 41). Reported percent abundances are based on the total terrestrial pollen sum excluding *Pinus* due to overrepresentation and potential long-distance transport of this taxon. The pollen percentage sum is based on a mean of 533 (including *Pinus*) and 253 grains/sample (excluding *Pinus*). The reported deciduous oak abundances (*SI Appendix*, Figs. S1 and S6) are represented by the combined percentages of *Quercus robur* and *Q. cerris*–types sensu Beug et al. (73). Deciduous oak abundances are commonly used as indicators for mid-elevation, relatively humid forest across the Mediterranean region (e.g., refs. 21, 74, 75). Assemblage change over time was summarized through DCA incorporated in past version 3.21 (76) on all upland tree and herb taxa >1% (*SI Appendix*, Figs. S3 and S4). Centroid values provide a mean axis score for each pollen zone (*SI Appendix*, Fig. S3).

Tree Richness Estimates. Palynological detection of rare taxa, and therefore richness estimates, is generally considered problematic as sample counts are commonly around 300 grains, and samples span different lengths of time, often have poor pollen preservation, and an overrepresentation of few pollen taxa (13). Richness counts rarefied to a common count sum (61) partly resolves these issues, but information is lost in the process since the sample richness is scaled back to the sample with the lowest counts sum, which limits the signal. Our approach uses SAC (77), which effectively bin sets of samples within a window to amplify the total pollen sum for the taxa richness estimate. Subsequently, the window is shifted up one sample and richness is recalculated, a process which is repeated along the entire record. We limited the analysis to tree taxa only since forest dynamics is our principal interest. Also, the majority of tree taxa in this region are wind pollinated, producing abundant pollen. Pollen types are well described (73) and misidentification is therefore minimal. Uncertain identifications were binned into larger taxonomical units (into Hamamelidaceae, *Alnus*, *Tsuga*, and *Picea* types) prior to the diversity analysis. The curve of cumulative tree richness levels off as more samples are added (78). The exact shape of the SAC depends on species evenness (77) and therefore on vegetation structure. To address these effects, overlapping SACs of up to 25 samples were constructed, based on all available pollen counts, to determine the appropriate sample window size at which the richness reaches an approximately stable value. The applied method pools the frequency of species relative to sample size (Kindt's exact accumulator, function "specaccum" in the R-package vegan 2.5 to 5; ref. 79). Based on the overlapping SACs (*SI Appendix*, Fig. S2), minimum, optimal, and maximum window sizes were selected of, respectively, 10, 15, and 20 samples (Fig. 3). Larger window sizes increase the total taxa count marginally (see *Methods* and *SI Appendix*, Fig. S2) but also result in loss of resolution. We therefore consider the window size of 15 as the optimal reflection of richness in both resolution and confidence between the pollen zones.

Tree pollen richness values for each of the window sizes were subsequently calculated based on the "collector" method that adds successive samples as they occur for a 1-step sliding window of variable size along the entire sequence. Corresponding ages are based on the midpoint of the respective window size. Our approach effectively estimates richness based on a large cumulative count sum of over 5,000 grains sample^{-1} and ensures a comparison between forest elements only. In addition, minimal sample-specific bias due to the high cumulative sums lead to optimal representation of rare taxa occurrences at pollen-zone resolution (78). To enable comparison of the SAC-based richness estimates, we show rarefaction analysis in *SI Appendix*, Fig. S4, computed with the "rarefy" function in the R-package vegan 2.5 to 5 (79). To limit the effect of low pollen counts in glacial samples on the rarefaction results, we have omitted samples with <150 tree pollen from the analysis. The expected number of taxa, E(T_{150}), and associated 95% CI are therefore based on the common value of 150 in 533 samples (*SI Appendix*, Fig. S4). The rarefaction analysis highlights high-resolution changes while the SAC were more robust and reflective of long-term change since the taxa count reach saturation (*SI Appendix*, Fig. S2). The pollen source area and resulting richness is influenced by the lake size (78), which, due to lake-level variations, could have varied in the early part of the record (38).

The reconstructed tree taxa richness represents the Ohrid catchment per pollen zone at a taxonomical resolution typical for pollen analysis, that is, at genus level. All tree taxa recorded as pollen in the uppermost sediments are present in the current LO catchment area (Global Biodiversity Information Facility data October 2020). For instance, sparse grains of *Picea*, *Betula*, and *Tilia* pollen are mirrored by the limited distribution of these species in the present vegetation (37), while significant *Pinus*, *Q. robur*–type, *Q. cerris*–type, *Q. ilex*–type, *Carpinus*, *Ostrya*, and *Abies* pollen abundances reflect local tree populations in the catchment today. This adds confidence that down-core records reflect actual presence of taxa in the catchment.

Time Series Analysis. Time series analyses for *Abies* and *Pinus* (*SI Appendix*, Fig. S6) follow the approach reported for deciduous oaks and total AP in Wagner et al. (33). Data series were resampled at regular intervals (linear interpolation) and submitted to continuous wavelet transform (Morlet window) incorporated in PAST version 3.21 software (76). In addition, phase relations were calculated using cross correlation (80) for three time periods: 0 to 500 ka, 500 to 940 ka, and 940 to 1,320 ka, representing the periods approximately prior, during, and following the EMPT. We limited the analysis to selected abundant tree taxa (*Abies, Pinus, Carpinus*, Cupressaceae [excluding *Taxodium*-type], and sclerophyllous oaks) and NAP, for which significant phase relations are determined relative to maximum deciduous oak abundance (*Q. cerris*–type and *Q. robur*–type) in each period. Negative numbers indicate a mean lead with respect to deciduous oak abundance and positive a lag.

Legacy Effects. To test for possible legacy at LO, we regressed zone-averaged pollen composition data and tree richness values against climate proxy data. Following Herzschuh et al. (69), we use the LR04 global benthic $\delta^{18}O$ stack (24) as a measure of glacial intensity. We regressed minimum, maximum, and mean $\delta^{18}O$ of contemporaneous and preceding stages (based on 2 kyr interpolated values from LR04) against the pollen-zone average values from the first DCA axis, representing the principal compositional changes in the vegetation proxy record (Fig. 2).

Data Availability. All study data are included in the article and/or supporting information. Previously published climate model data were used for this work (https://doi.org/10.1594/PANGAEA.901055) (67).

ACKNOWLEDGMENTS. The Scientific Collaboration on Past Speciation Conditions in LO drilling project was funded by the International Continental Scientific Drilling Program, the German Ministry of Higher Education and Research, the German Research Foundation, the University of Cologne, the British Geological Survey, the Istituto Nazionale di Geofisica e Vulcanologia and Consiglio Nazionale delle Ricerche (both Italy), and the governments of the republics of North Macedonia and Albania. T.D. wishes to acknowledge Margot Cramwinckel for assisting with R coding and Giovanni Dammers for sample preparation. K.P. and A.K. acknowledge financial support by the German Research Foundation (DFG Grants PA 2664/2-1, PA 2664/2-2, and KO4960/1). We thank two anonymous reviewers for their detailed comments that helped improve the manuscript.

1. R. F. Noss, Beyond Kyoto: Forest management in a time of rapid climate change. *Conserv. Biol.* **15**, 578–590 (2001).
2. P. Taberlet, R. Cheddadi, Ecology. Quaternary refugia and persistence of biodiversity. *Science* **297**, 2009–2010 (2002).
3. T. P. Dawson, S. T. Jackson, J. I. House, I. C. Prentice, G. M. Mace, Beyond predictions: Biodiversity conservation in a changing climate. *Science* **332**, 53–58 (2011).
4. R. T. Corlett, D. A. Westcott, Will plant movements keep up with climate change? *Trends Ecol. Evol.* **28**, 482–488 (2013).
5. P. C. Tzedakis, Seven ambiguities in the Mediterranean palaeoenvironmental narrative. *Quat. Sci. Rev.* **26**, 2042–2066 (2007).
6. C. Reid, E. M. Reid, "The Pliocene flora of the Dutch-Prussian border" in *Mededeelingen van de Rijksopsporing van Delfstoffen*, M. Nijhoff, Ed. (Gravenhage, 1915), pp. 1–178.
7. T. Van der Hammen, T. A. Wijmstra, W. H. Zagwijn, "The floral record of the late cenozoic of Europe" in *The Late Cenozoic Glacial Ages*, K. K. Turekian, Ed. (Yale University, 1971), pp. 391–424.
8. J.-C. Svenning, Deterministic Plio-Pleistocene extinctions in the European cool-temperate tree flora. *Ecol. Lett.* **6**, 646–653 (2003).
9. B. Frenzel, The Pleistocene vegetation of Northern Euras. *Science* **161**, 637–649 (1968).
10. K. D. Bennett, P. C. Tzedakis, K. J. Willis, Quaternary refugia of North European trees. *J. Biogeogr.* **18**, 103–115 (1991).
11. B. Huntley, Species-richness in north-temperate zone forests. *J. Biogeogr.* **20**, 163–180 (1993).
12. K. J. Willis, R. J. Whittaker, Perspectives: Paleoecology. The refugial debate. *Science* **287**, 1406–1407 (2000).
13. D. Magri, F. Di Rita, J. Aranbarri, W. Fletcher, P. González-Sampériz, Quaternary disappearance of tree taxa from Southern Europe: Timing and trends. *Quat. Sci. Rev.* **163**, 23–55 (2017).
14. F. Médail, K. Diadema, Glacial refugia influence plant diversity patterns in the Mediterranean Basin. *J. Biogeogr.* **36**, 1333–1345 (2009).
15. J.-P. Suc, Origin and evolution of the Mediterranean vegetation and climate in Europe. *Nature* **307**, 429–432 (1984).
16. A. Bertini, Pollen record from Colle Curti and Cesi: Early and Middle Pleistocene mammal sites in the Umbro-Marchean Apennine Mountains (Central Italy). *J. Quat. Sci* **15**, 825–840 (2000).
17. S. Joannin, F. Bassinot, N. C. Nebout, O. Peyron, C. Beaudouin, Vegetation response to obliquity and precession forcing during the Mid-Pleistocene Transition in Western Mediterranean region (ODP site 976). *Quat. Sci. Rev.* **30**, 280–297 (2011).
18. C. Ravazzi *et al*., The lacustrine deposits of Fornaci di Ranica (late Early Pleistocene, Italian Pre-Alps): Stratigraphy, palaeoenvironment and geological evolution. *Quat. Int.* **131**, 35–58 (2005).
19. A. Bertini, Pliocene to Pleistocene palynoflora and vegetation in Italy: State of the art. *Quat. Int.* **225**, 5–24 (2010).
20. D. Biltekin *et al*., Anatolia: A long-time plant refuge area documented by pollen records over the last 23 million years. *Rev. Palaeobot. Palynol.* **215**, 1–22 (2015).
21. N. Combourieu-Nebout, Climate changes in the central Mediterranean and Italian vegetation dynamics since the Pliocene. *Rev. Palaeobot. Palynol.* **218**, 127–147 (2015).
22. M. J. Head, P. Gibbard, Early–Middle Pleistocene transitions: Linking terrestrial and marine realms. *Quat. Int.* **389**, 7–46 (2015).
23. N. J. Shackleton, N. D. Opdyke, Oxygen-isotope and paleomagnetic stratigraphy of Pacific core V28–239: Late Pliocene to latest Pleistocene. *Geol. Soc. Am.* **145**, 449–464 (1976).
24. L. E. Lisiecki, M. E. Raymo, A Pliocene-Pleistocene stack of 57 globally distributed benthic $\delta^{18}O$ records. *Paleoceanography* **20**, PA1003 (2005).
25. P. U. Clark *et al*., The middle Pleistocene transition: Characteristics, mechanisms, and implications for long-term changes in atmospheric pCO_2. *Quat. Sci. Rev.* **25**, 23–24 (2006).
26. R. Bintanja, R. S. van de Wal, North American ice-sheet dynamics and the onset of 100,000-year glacial cycles. *Nature* **454**, 869–872 (2008).
27. B. Hönisch, N. G. Hemming, D. Archer, M. Siddall, J. F. McManus, Atmospheric carbon dioxide concentration across the mid-Pleistocene transition. *Science* **324**, 1551–1554 (2009).
28. H. Elderfield *et al*., Evolution of ocean temperature and ice volume through the mid-Pleistocene climate transition. *Science* **337**, 704–709 (2012).
29. E. McClymont, S. M. Sosdian, A. Rosell-Melé, Y. Rosenthal, Pleistocene sea-surface temperature evolution: Early cooling, delayed glacial intensification, and implications for the mid-Pleistocene climate transition. *Earth Sci. Rev.* **123**, 173–193 (2013).
30. P. C. Tzedakis, M. Crucifix, T. Mitsui, E. W. Wolff, A simple rule to determine which insolation cycles lead to interglacials. *Nature* **542**, 427–432 (2017).
31. K. J. Willis, K. J. Niklas, The role of Quaternary environmental change in plant macroevolution: The exception or the rule? *Philos. Trans. R. Soc. Lond. B Biol. Sci.* **359**, 159–172 (2004), discussion 172.
32. A. Francke *et al*., Sedimentological processes and environmental variability at Lake Ohrid (Macedonia, Albania) between 637 ka and the present. *Biogeosciences* **13**, 1179–1196 (2016).
33. B. Wagner *et al*., Mediterranean winter rainfall in phase with African monsoons during the past 1.36 million years. *Nature* **573**, 256–260 (2019).
34. B. Huntley, H. J. B. Birks, *An Atlas of Past and Present Pollen Maps for Europe: 0-13,000 Years Ago* (Cambridge University Press, 1983), pp. 667.
35. P. C. Tzedakis, Long-term tree populations in northwest Greece through multiple Quaternary climatic cycles. *Nature* **364**, 437–440 (1993).
36. K. J. Willis, The vegetational history of the Balkans. *Quat. Sci. Rev.* **13**, 769–788 (1994).
37. L. Sadori *et al*., Pollen-based paleoenvironmental and paleoclimatic change at Lake Ohrid (south-eastern Europe) during the past 500 ka. *Biogeosciences* **13**, 1423–1437 (2016).
38. K. Panagiotopoulos *et al*., Insights into the evolution of the young Lake Ohrid ecosystem and vegetation succession from a southern European refugium during the Early Pleistocene. *Quat. Sci. Rev.* **227**, 106044 (2020).
39. V. Matevski, *Forest Vegetation of Galièica Mountain Range in Macedonia* (Založba ZRC Press, Ljubljana, 2011), pp. 200.
40. K. Panagiotopoulos, A. Aufgebauer, F. Schäbitz, B. Wagner, Vegetation and climate history of the Lake Prespa region since the Lateglacial. *Quat. Int.* **293**, 157–169 (2013).
41. L. Sadori *et al*., Pollen-based paleoenvironmental and paleoclimatic change at Lake Ohrid (south-eastern Europe) during the past 500 ka. *Biogeosciences* **13**, 1423–1437, (2016). Correction in: Biogeosciences, https://doi.org/10.5194/bg-13-1423-2016-corrigendum (2018).
42. I. Kousis *et al*., Centennial-scale vegetation dynamics and climate variability in SE Europe during Marine Isotope Stage 11 based on a pollen record from Lake Ohrid. *Quat. Sci. Rev.* **190**, 20–38 (2018).
43. G. Sinopoli *et al*., Palynology of the last interglacial complex at Lake Ohrid: Palaeoenvironmental and palaeoclimatic inferences. *Quat. Sci. Rev.* **180**, 177–192 (2018).
44. A. Koutsodendris, I. Kousis, O. Peyron, B. Wagner, J. Pross, The Marine Isotope Stage 12 pollen record from Lake Ohrid (SE Europe): Investigating short-term climate change under extreme glacial conditions. *Quat. Sci. Rev.* **221**, 105873 (2019).
45. G. Sinopoli *et al*., Pollen-based temperature and precipitation changes in the Ohrid Basin (western Balkans) between 160 and 70 ka. *Clim. Past* **15**, 53–71 (2019).
46. T. Wilke *et al*., Deep drilling reveals massive shifts in evolutionary dynamics after formation of ancient ecosystem. *Sci. Adv.* **6**, eabb2943 (2020).
47. N. Hoffmann, K. Reicherter, T. Fernández-Steeger, C. Grützner, Evolution of ancient Lake Ohrid: A tectonic perspective. *Biogeosciences* **7**, 3377–3386 (2010).
48. U. Herzschuh, Reliability of pollen ratios for environmental reconstructions on the Tibetan Plateau. *J. Biogeogr.* **34**, 1265–1273 (2007).
49. P. C. Tzedakis *et al*., Interglacial diversity. *Nat. Geosci.* **2**, 751–755 (2009).
50. J. H. C. Bosmans *et al*., Precession and obliquity forcing of the freshwater budget over the Mediterranean. *Quat. Sci. Rev.* **123**, 16–30 (2015).
51. R. Orain, V. Lebreton, E. Russo Ermolli, N. Combourieu-Nebout, A.-M. Sémah, *Carya* as marker for tree refuges in southern Italy (Boiano basin) at the Middle Pleistocene. *Palaeogeogr. Palaeoclimatol. Palaeoecol.* **369**, 295–302 (2013).
52. D.-D. Rousseau *et al*., Long-distance pollen transport from North America to Greenland in spring. *J. Geophys. Res.* **113**, G02013 (2008).
53. N. Leicher *et al*., Central Mediterranean explosive volcanism and tephrochronology during the last 630 ka based on the sediment record from Lake Ohrid. *Quat. Sci. Rev.* **226**, 106021 (2019).
54. B. Wagner *et al*., The environmental and evolutionary history of Lake Ohrid (FYROM/Albania) - Interim results from the SCOPSCO deep drilling project. *Biogeosciences* **14**, 2033–2054 (2017).
55. T. Wijmstra, Palynology of the first 30 metres of a 120 m deep section in northern Greece. *Acta Bot. Neerl.* **18**, 511–527 (1969).
56. T. Wijmstra, A. Smit, Palynology of the middle part (30-78 metres) of the 120 m deep section in northern Greece (Macedonia). *Acta Bot. Neerl.* **25**, 297–312 (1976).
57. A. Van der Wiel, T. Wijmstra, Palynology of the lower part (78-120 m) of the core Tenaghi Philippon II, Middle Pleistocene of Macedonia. Greece. *Rev. Palaeobot. Palynol.* **52**, 73–88 (1987).
58. A. Van der Wiel, T. Wijmstra, Palynology of the 112.8-197.8 m interval of the core Tenaghi Philippon III, Middle Pleistocene of Macedonia. *Rev. Palaeobot. Palynol.* **52**, 89–117 (1987).
59. W. H. Zagwijn, The beginning of the ice age in Europe and its major subdivisions. *Quat. Sci. Rev.* **11**, 583–591 (1992).
60. P. C. Tzedakis, H. Hooghiemstra, H. Pälike, The last 1.35 million years at Tenaghi Philippon: Revised chronostratigraphy and long-term vegetation trends. *Quat. Sci. Rev.* **25**, 3416–3430 (2006).
61. H. J. B. Birks, J. M. Line, The use of rarefaction analysis for estimating palynological richness from Quaternary pollen-analytical data. *Holocene* **2**, 1–10 (1992).
62. P. Samuelsson, E. Kourzeneva, D. Mironov, The impact of lakes on the European climate as simulated by a regional climate model. *Boreal Environ. Res.* **15**, 113–129 (2010).
63. M. Notaro *et al*., Influence of the Laurentian Great Lakes on regional climate. *J. Clim.* **26**, 789–804 (2013).
64. J. H. Lacey *et al*., Northern Mediterranean climate since the Middle Pleistocene: A 637 ka stable isotope record from Lake Ohrid (Albania/Macedonia). *Biogeosciences* **13**, 1801–1820 (2016).
65. K. H. Roucoux, P. C. Tzedakis, M. R. Frogley, I. T. Lawson, R. C. Preece, Vegetation history of the marine isotope stage 7 interglacial complex at Ioannina, NW Greece. *Quat. Sci. Rev.* **27**, 1378–1395 (2008).
66. K.-C. Emeis *et al*., Eastern Mediterranean surface water temperatures and $\delta^{18}O$ composition during deposition of sapropels in the late Quaternary. *Paleoceanography* **18**, 1005 (2003).
67. B. Wagner *et al*., Modeled climate time series data. Pangaea, https://doi.org/10.1594/PANGAEA.901055. Accessed 1 May 2021.
68. B. A. Davis *et al*., The European Modern Pollen Database (EMPD) project. *Veg. Hist. Archaeobot.* **22**, 521–530 (2013).
69. U. Herzschuh *et al*., Glacial legacies on interglacial vegetation at the Pliocene-Pleistocene transition in NE Asia. *Nat. Commun.* **7**, 11967 (2016).
70. H. Vogel, B. Wagner, G. Zanchetta, R. Sulpizio, P. Rosén, A paleoclimate record with tephrochronological age control for the last glacial–interglacial cycle from Lake Ohrid, Albania and Macedonia. *J. Paleolimnol.* **44**, 295–310 (2010).
71. J. Pross *et al*., The 1.35-Ma-long terrestrial climate archive of Tenaghi Philippon, northeastern Greece: Evolution, exploration, and perspectives for future research. *Newsl. Stratigr.* **48**, 253–276 (2015).

72. K. Faegri, J. Iversen, P. E. Kaland, K. Krzywinski, *Text Book of Pollen Analysis*(The Blackburn Press, NJ, ed. IV, 1989), pp. 328.
73. H.-J. Beug, *Leitfaden der Pollenbestimmung für Mitteleuropa und angrenzende Gebiete* (Verlag Dr. Friedrich Pfeil, München, Germany, 2004), pp. 542.
74. D. Langgut, A. Almogi-Labin, M. Bar-Matthews, M. Weinstein-Evron, M., Vegetation and climate changes in the South Eastern Mediterranean during the Last Glacial-Interglacial cycle (86 ka): New marine pollen record. *Quat. Sci. Rev.* **30**, 3960–3972 (2011).
75. M. Rossignol-Strick, The Holocene climatic optimum and pollen records of sapropel 1 in the Eastern Mediterranean, 9000–6000 BP. *Quat. Sci. Rev.* **18**, 515–530 (1999).
76. Ø. Hammer, D. A. T. Harper, P. D. Ryan, PAST: Paleontological statistics software package for education and data analysis. Palaeontologia Electronica 4, 9 (2001). https://palaeo-electronica.org/2001_1/past/issue1_01.htm PAST version 4.05 from https://www.nhm.uio.no/english/research/infrastructure/past/.
77. T. Giesecke, B. Ammann, A. Brande, Palynological richness and evenness: Insights from the taxa accumulation curve. *Veg. Hist. Archaeobot.* **23**, 217–228 (2014).
78. C. Y. Weng, H. Hooghiemstra, J. F. Duivenvoorden, Challenges in estimating past plant diversity from fossil pollen data: Statistical assessment, problems, and possible solutions. *Divers. Distrib.* **12**, 310–318 (2006).
79. J. Oksanen *et al*., Vegan: Community Ecology Package. R package version 2.5.6, https://cran.r-project.org/web/packages/vegan/index.html. Deposited 31 August 2019.
80. J. C. Davis, *Statistics and Data Analysis in Geology* (John Wiley & Sons, 1986), pp. 656.
81. K. Lindhorst *et al*., Sedimentary and tectonic evolution of Lake Ohrid (Macedonia/Albania). *Basin Res.* **27**, 84–101 (2015).
82. P. Wang, J. Tian, L. Lourens, Obscuring of long eccentricity cyclicity in Pleistocene oceanic carbon isotope records. *Earth Planet. Sci. Lett.* **290**, 319–330 (2010).
83. T. Y. M. Konijnendijk, M. Ziegler, L. J. Lourens, On the timing and forcing mechanisms of late Pleistocene glacial terminations: Insights from a new high-resolution benthic stable oxygen isotope record of the eastern Mediterranean. *Quat. Sci. Rev.* **129**, 308–320 (2015).